Discrete-time Modelling and Robust Analysis of a Buck Converter

Petar Iordanov [*] **Mark Halton** [**]

[*] *University of Limerick, Limerick, Ireland (e-mail: petar.iordanov@ul.ie).*
[**] *University of Limerick, Limerick, Ireland (e-mail: mark.halton@ul.ie)*

Abstract: A discrete-time state-space representation of a Buck converter is presented. This analytical state-space model provides explicit insight on how circuit parameters influence the stability and transient performance for this converter type. Variations in the power rail components and parasitic resistances are accommodated, which are typically neglected in compensator synthesis for switched mode power supplies. With this representation, robust stability and feedback performance can be readily assessed. Moreover, the model can be employed directly for the design of digital robust compensators, and it provides a basis for the development of compensators in analytical form rather than the use of numerical discretisation techniques.

1. INTRODUCTION

Application trends in power conversion require multiple rails, multiple phases and advanced power management, which must be regulated to a high degree of voltage accuracy. Traditionally, analogue power management integrated circuits have performed this task, but the industry is moving towards power architectures which are smaller and more efficient. The requirement for an increasing number of power rails and the economics of digital and analogue IC production are factors which are influencing the shift towards digital power controllers. However, a significant number of digital compensators are still designed through numerical discretisation of their continuous-time counterparts. Generally speaking, these compensators may not be optimal due to the nature of the employed design methodologies and the approximation methods used. Furthermore, this type of approach does not allow for analytical digital control design methods which may be more suited for the multi-rail/multi-phase paradigm. In addition the relationship of the parameters in the model, in particular the power rail components, is lost during the conversion into the discrete-time domain.

In most compensator design techniques for power conversion applications such as *switched mode power supplies* (SMPS), the component/parameter variation is not taken into account. Besides the manufacturing tolerances alone, component values often vary during operation. Generally, the power rail components and parasitic estimates are set at nominal fixed values. While a compensator design may work perfectly with the nominal component set, deterioration in performance may prove significant when using the actual component values, and in some cases, instability in the feedback loop may occur. The inclusion of parametric variation will not only allow to estimate the stability and transient performance of an already designed compensator, but will also enable the use of robust control designs that can tolerate the factory-rated components variations while providing satisfactory transient performance over a large operating range. Linear robust compensators are fixed and time-invariant, and can be readily implemented in a digitally-controlled configuration. Computational effort of robust compensators is insignificant compared to optimisation-based adaptive algorithms and model-predictive control algorithms. The use of high frequency sampling and switching, makes the latter two control algorithms very difficult to implement in embedded applications.

This paper proposes an analytical discrete-time parametrised model that incorporates the sample frequency, modulator effects, delays in the control loop and variations in the power rail components. An obvious advantage of using an analytical discrete-time model is that control loops can be modelled directly in the digital domain. The small-signal state-space modelling approach presented by Maksimović and Zane [2007], is exploited in this work. The robust discrete-time analytical model detailed should be distinguished from SMPS models presented in earlier publications, where only numerical state-space representations have been provided; for example, Bu et al. [1997], Sanchez-Peña and Sznaier [1998]. The introduction of parametric uncertainty does not alter the linearity of the model, and enables various types of analyses to be directly employed. The analytical model representation is ideally suited to quantify the influence of parameter variation using well-developed robustness analysis techniques. This model description also accommodates the design of robust digital compensators in analytical form.

This paper is outlined as follows: in Section 2 an analytical discrete-time state-space model for a Buck converter is derived with the corresponding matrices provided in an appendix. Section 3 details a case study example with robustness analysis results for this strictly real parametric uncertainty problem. Concluding remarks and an outline of future work is given in Section 4.

2. DISCRETE-TIME ANALYTICAL MODEL WITH PARAMETRIC UNCERTAINTY

2.1 Analytical Discretisation

A continuous-time model is generally represented in state-space in the following form:

$$\begin{aligned}\dot{x}(t) &= Ax(t) + Bu(t)\\ y(t) &= Cx(t) + Du(t)\end{aligned} \tag{1}$$

The discrete-time state equation is normally expressed by

$$x[n+1] = e^{AT_s}x[n] + \left(\int_0^{T_s} e^{A\nu}dv\right)Bu[n] \tag{2}$$

where T_s is the sample time and $\nu = nT_s + T_s - \tau$.

Exact discretisation may sometimes be intractable due to the heavy matrix exponential and integral operations involved. It is much easier to calculate an approximate discrete model based on that for small time-steps $e^{AT_s} \approx I + AT_s$. The approximate solution then becomes

$$x[n+1] \approx \underbrace{(I + AT_s)}_{\Phi}x[n] + \underbrace{(IT_s + \frac{1}{2}AT_s^2)B}_{\Gamma}u[n] \tag{3}$$

and the discrete-time state space model is given by

$$\begin{aligned}x[n+1] &= \Phi x[n] + \Gamma u[n]\\ y[n] &= Cx[n]\end{aligned} \tag{4}$$

2.2 Discrete-time Modelling of a Buck Converter

Modeling of a single-phase SMPS is studied in this paper. SMPS is an electronic power supply that incorporates a switching regulator to efficiently convert electrical power. An SMPS is usually employed to provide a regulated output voltage, typically at a level different from the input voltage. Unlike a linear power supply, the pass transistor of a switching mode supply switches very quickly (typically between 50kHz and 1 MHz) between full-on and full-off states, which minimises energy loss. There are different topologies and modes of operation available for switched-mode power supplies, and for this work a Buck SMPS operating in continuous-conduction mode with a resistive load is studied, Erickson and Maksimović [2001]. A typical single-phase Buck converter with digital voltage-mode control is illustrated in Figure 1.

The A/D converter samples the output voltage error at the sampling rate equal to the switching frequency f_s. There are two samplers in the feedback loop: A/D converter (sampling of the error voltage), and the *digital pulse-width modulator* (DPWM). The DPWM works at a much higher frequency than the A/D converter (e.g. 25.6MHz, 51.2MHz etc.). As a result, the system small-signal model does not include a sample-and-hold. Instead, the relationship between the small-signal perturbations of the voltage error signal and the duty-cycle $d[n]$ includes a delay t_d between the A/D sampling at $t_s = nT_s$ and the modulator sampling at t_p. It is assumed that the total delay is shorter than the switching period T_s, i.e. $0 < t_d < T_s$. Assuming that $t_d = \frac{T_s}{2}$, (3) can be rewritten as

$$x[n+1] \approx (I + AT_s)\,x[n] + (I + A(T_s - t_d))\,T_sBu[n] \tag{5}$$

In each state of the switch, *1* or *2*, the converter circuit is linear and time-invariant. To simplify the modelling, losses due to parasitic resistance are neglected except for the dominant effect of the capacitor ESR, R_C, as well as R_L. With that in mind, the continuous-time state-space representation is given by, Maksimović and Zane [2007]:

$$\begin{aligned}
x(t) &= \begin{bmatrix} v(t)\\ i(t)\end{bmatrix}, \quad u(t) = d(t), \quad y(t) = v_{out}(t)\\
A &= \begin{bmatrix} \dfrac{-1}{(R+R_C)C} & \dfrac{R}{(R+R_C)C}\\ \dfrac{-R}{(R+R_C)L} & -\left(R_L + \dfrac{R_CR}{R_C+R}\right)\dfrac{1}{L}\end{bmatrix}\\
B &= \begin{bmatrix} 0\\ \dfrac{1}{L}\end{bmatrix}\\
C &= \begin{bmatrix} \dfrac{R}{R+R_C} & \dfrac{R_CR}{R_C+R}\end{bmatrix}
\end{aligned} \tag{6}$$

where d is the duty cycle of the signal c that drives the switch. The state variables are: v - the voltage across the capacitor C, and i - the current through the inductor L. The output variable is the voltage across the load, v_{out}.

Assuming that $R_C \ll R$, the model of (6) is discretised using the approximation of (3), and the state equation matrices are

$$\begin{aligned}\Phi &= e^{AT_s} \approx I + AT_s\\ \Gamma &= e^{A(T_s - t_d)}BV_gT_s \approx (I + A\,(T_s - t_d))\,BV_gT_s\end{aligned} \tag{7}$$

From (7), the discrete state-space matrices are derived:

$$\begin{aligned}
\Phi &= \begin{bmatrix} 1 - \dfrac{T_s}{RC} & \dfrac{T_s}{C}\\ \dfrac{-T_s}{L} & 1 - \dfrac{T_sR_C}{L}\end{bmatrix}\\
\Gamma &= \begin{bmatrix} \dfrac{(T_s - t_d)\,V_gT_s}{LC}\\ \dfrac{V_gT_s}{L} - \dfrac{(T_s - t_d)\,V_gT_sR_C}{L^2}\end{bmatrix}
\end{aligned} \tag{8}$$

2.3 Incorporation of Parametric Uncertainty in the Model

Variation in the circuit parameters R, L, C, R_L and R_C are represented using the canonical representations:

$$\begin{aligned}
R &= R_0\,(1 + w_R\delta_R)\\
L &= L_0\,(1 + w_L\delta_L)\\
C &= C_0\,(1 + w_C\delta_C)\\
R_L &= R_{L_0}\,(1 + w_{R_L}\delta_{R_L})\\
R_C &= R_{C_0}\,(1 + w_{R_C}\delta_{R_C})
\end{aligned} \tag{9}$$

where R_0, L_0, C_0 and R_{C_0} are the nominal values of the components, while w_R, w_L, w_C, w_{R_L}, and w_{R_C} are weighting coefficients representing the size of component variations. Additional normalised varying parameters, $\delta_i \in [-1, 1]$, are introduced to account for the parametric variations.

An analytical discrete-time state-space model is derived from (8)-(9). The model is produced by building an equivalent block diagram, where uncertain/varying parameters are represented in the way illustrated in Figure 2. The block diagram is then restructured via a *linear fractional transformation*, (LFT), Doyle et al. [1991], where all uncertainty parameters are extracted and contained within an overall uncertainty block (Δ), as shown in Figure 3.

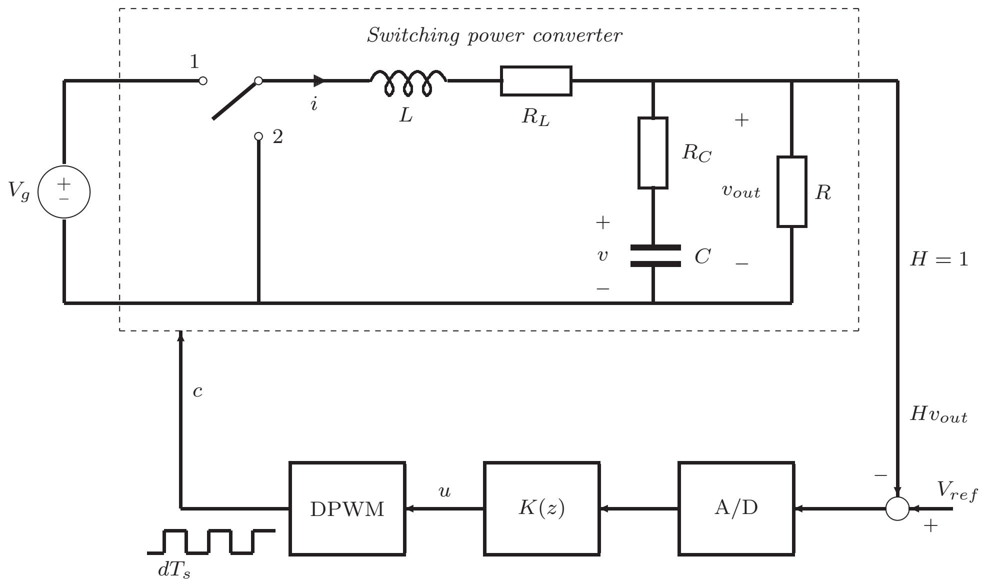

Fig. 1. Buck Converter with Digital Control.

The block diagram of the model is presented in Figure 4. Note that most component parameters appear multiple times in the block diagram, i.e. *repeated uncertainty* blocks are present. By removing the δ_i blocks from the diagram, additional inputs (u_{Δ_i}) and outputs (y_{Δ_i}) are incorporated in the model description given by

$$\begin{bmatrix} \hat{x}[n+1] \\ \hline y_\Delta[n] \\ y[n] \end{bmatrix} = \underbrace{\left[\begin{array}{c|cc} \Phi & \Gamma_\Delta & \Gamma \\ \hline C_\Delta & D_{11} & D_{12} \\ C & D_{21} & D \end{array}\right]}_{M} \begin{bmatrix} \hat{x}[n] \\ \hline u_\Delta[n] \\ u[n] \end{bmatrix}$$
$$\begin{bmatrix} y_\Delta(z) \\ y(z) \end{bmatrix} = \underbrace{\begin{bmatrix} M_{11}(z) & M_{12}(z) \\ M_{21}(z) & M_0(z) \end{bmatrix}}_{M(z)} \begin{bmatrix} u_\Delta(z) \\ u(z) \end{bmatrix} \tag{10}$$

where

$$\begin{aligned} u_\Delta =& [u_{L_1},\ u_{L_2},\ u_{L_3},\ u_{L_4},\ u_{C_1},\ u_{C_2}, \ldots \\ & u_{C_3},\ u_R,\ u_{R_{L1}},\ u_{R_{L2}},\ u_{R_{C1}},\ u_{R_{C2}}] \\ y_\Delta =& [y_{L_1},\ y_{L_2},\ y_{L_3},\ y_{L_4},\ y_{C_1},\ y_{C_2}, \ldots \\ & y_{C_3},\ y_R,\ y_{R_{L1}},\ y_{R_{L2}},\ y_{R_{C1}},\ y_{R_{C2}}] \\ \Delta =& diag\{\delta_L I_4,\ \delta_C I_3,\ \delta_R,\ \delta_{R_L} I_2,\ \delta_{R_C} I_2\} \end{aligned} \tag{11}$$

The state space matrices Γ_Δ, C_Δ, D_{11}, D_{12} and D_{21} are given in Appendix A. In the $\mathcal{Z}$-domain, the LFT of the augmented model, $M(z)$, and component variation matrix, Δ, is described by:

$$\begin{aligned} G(z) &= \mathcal{F}_u(M(z), \Delta) = \\ &= M_0(z) + M_{21}(z)\Delta\left(I - M_{11}(z)\Delta\right)^{-1} M_{12}(z) \end{aligned} \tag{12}$$

The interconnection of Figure 3 is the standard structure employed in the analysis of robust stability of models subject to parametric uncertainty. The discrete-time LFT model of a Buck converter is in a form suitable for robustness analysis in Matlab, and it has been verified against the continuous-time model presented in Halton et al. [2008].

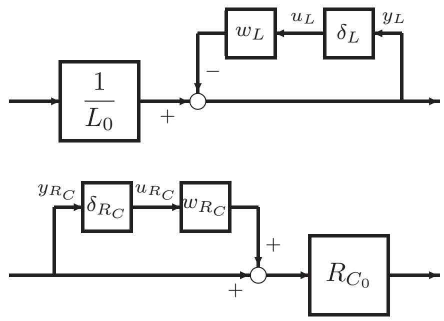

Fig. 2. Representation of Parametric Uncertainty.

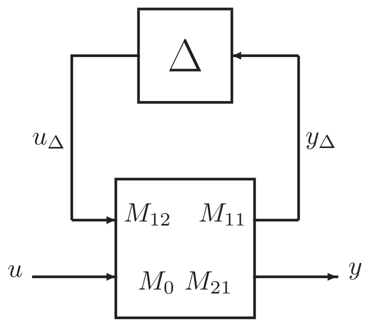

Fig. 3. Upper LFT of $M(z)$ and Δ.

3. ROBUSTNESS ANALYSIS

The discrete state-space model derived in the previous section is now used with the component values and variations presented in Table 1. For this model, the input voltage $V_g = 12V$, sample time $T_s = 1\mu s$ and loop delay $t_d = 500ns$. A discrete-time controller was designed using a *model-predictive control* (MPC) technique outlined in Rossiter [2003]. The control technique uses three design parameters: control horizon, n_u , output horizon, n_y, and cost scaling factor, λ. The synthesis produces a fixed

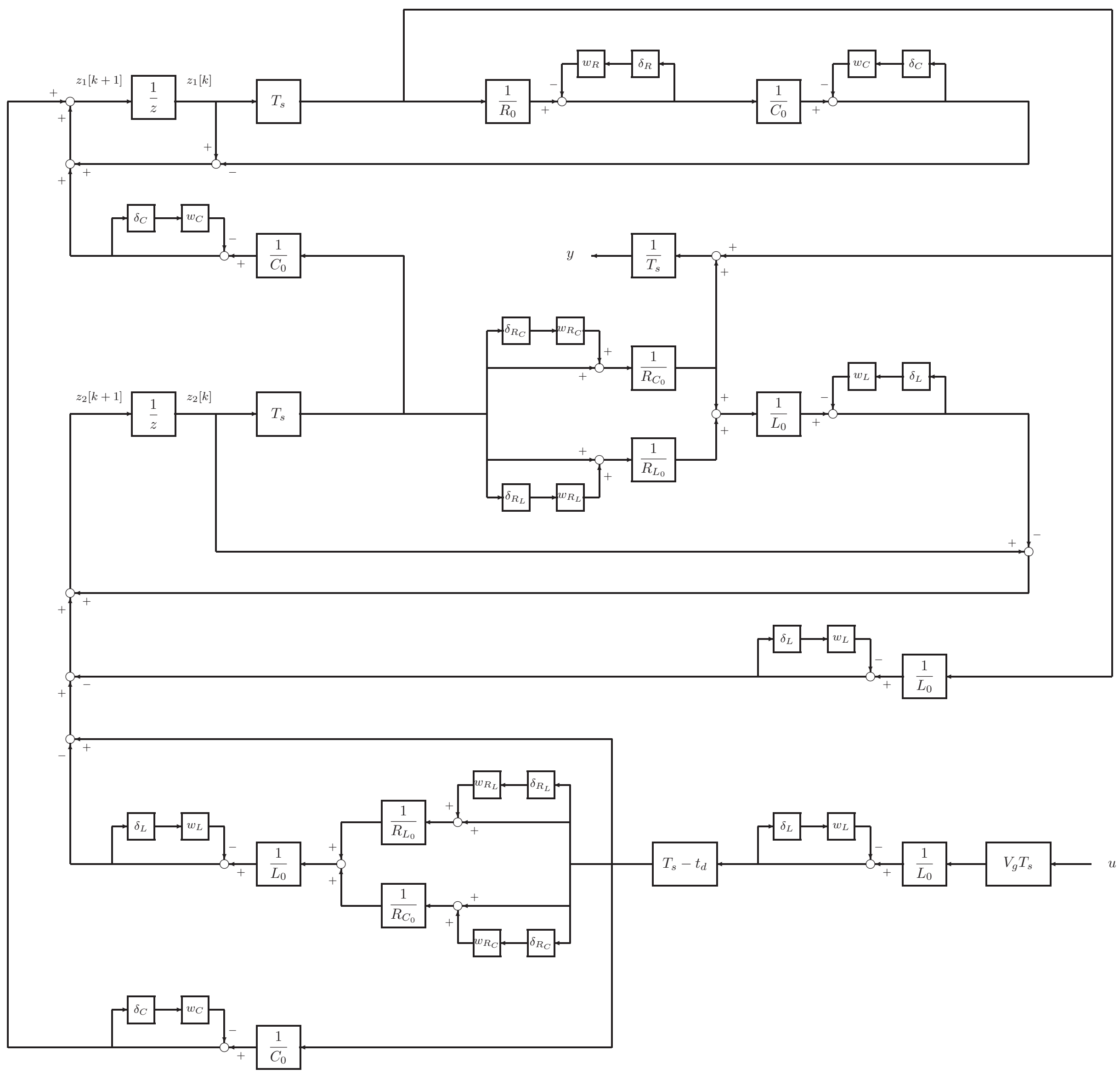

Fig. 4. Discrete-Time Model with Parametric Uncertainty.

Parameter	Nominal Value	Variation
R	$R_0 = 1.6\Omega$	$\pm 50\% \Rightarrow w_R = 0.5$
L	$L_0 = 500nH$	$\pm 35\% \Rightarrow w_L = 0.35$
C	$C_0 = 470\mu F$	$\pm 40\% \Rightarrow w_C = 0.4$
R_L	$R_{L_0} = 25m\Omega$	$\pm 25\% \Rightarrow w_{R_L} = 0.25$
R_C	$R_{C_0} = 3m\Omega$	$\pm 25\% \Rightarrow w_{R_C} = 0.25$

Table 1. Model Parameters.

discrete-time SISO controller that stabilises the nominal plant. The designed controller is described by

$$K(z) = \frac{4.969z^4 - 5.196z^3 + 0.5733z^2}{z^4 - 0.8928z^3 - 0.2125z^2 + 0.1053z} \qquad (13)$$

It was verified that the poles of the nominal closed-loop system are all inside the unit circle. Robustness is assessed using the *structured singular value*, which is normally denoted by μ, Doyle [1982]. As the μ calculation is an $\mathcal{NP}$-hard problem, lower and upper bounds are generally computed over a grid of frequencies. Moreover, for *real* parametric uncertainty, i.e. $\delta_i \in \mathcal{R}$, μ may be discontinuous and the gap between the bounds may become significant, Barmish et al. [1990]. A number of discrete-time robustness analysis algorithms are available to provide non-conservative estimates of the robust stability margin for this strictly real uncertainty problem formulation, with the following three algorithms (one upper bound and two lower bound) used in this analysis:

- μ_u^1: μ-Tools upper bound (using the "greatest accuracy" option). This is the frequency-gridding algorithm implemented in MATLAB's *Robust Control Toolbox*, Balas et al. [2010].
- μ_l^1: *basic optimisation approach* (BOA) for μ lower bound, outlined in Hayes and Iordanov [2000]. A frequency-gridding approach which generally provides very good estimates of the μ lower bound.
- μ_l^2: *pole placement approach* (PPA) for μ lower bound, outlined in Iordanov et al. [2003]. A frequency-independent approach which returns a μ lower bound quickly and accurately.

The first two algorithms use a grid of 500 points spaced logarithmically in the frequency interval $\omega \in [10^5,\ 10^7]\ rad/s$. The robustness analysis results are presented in Table 2 and illustrated in Figure 5.

The analysis results presented in Table 2 indicate that the discrete-time system in not robustly stable as both μ lower and upper bounds are larger than unity. It is noteworthy to point out that the μ_l^2 lower bound is larger than the μ upper bound detected from the frequency grid search, μ_u^1. This comes as no surprise, bearing in mind the discrete nature of the frequency grid search. Both lower bound algorithms, μ_l^1 and μ_l^2, returned a worst-case destablising set of parameters $\{\delta_R^{wc}, \delta_L^{wc}, \delta_C^{wc}, \delta_{R_L}^{wc}, \delta_{R_C}^{wc}\}$. The impact of each uncertain parameter on the robust stability and performance can be assessed by calculating the μ-sensitivities, Braatz and Morari [1991].

The component/parameter values that cause the closed-loop system to become unstable are calculated using the expressions of (9) and listed in Table 3. The controller $K(z)$ provides nominal closed-loop stability, but it fails to ensure robust stability as parameter variations are not taken into account in the MPC design.

	μ Algorithm		
	μ_u^1	μ_l^1	μ_l^2
$\mu(\omega_p)$	1.0056	1.0055	1.0085
$\omega_p\ [rad/s]$	5.3144×10^5	5.3144×10^5	5.2961×10^5
δ_L^{wc}	-	0.9722	0.9916
δ_C^{wc}	-	-0.9946	-0.9916
δ_R^{wc}	-	0.9924	0.9916
$\delta_{R_L}^{wc}$	-	-0.9943	-0.9916
$\delta_{R_C}^{wc}$	-	-0.9946	-0.9916

Table 2. μ-Analysis Results.

Parameter	Value from μ_l^1	Value from μ_l^2
R	2.394Ω	2.393Ω
L	$670.1nH$	$673.5nH$
C	$283\mu F$	$283.6\mu F$
R_L	$18.8m\Omega$	$18.8m\Omega$
R_C	$2.25m\Omega$	$2.26m\Omega$

Table 3. Destabilising Parameters.

4. CONCLUSION

A discrete-time state-space analytical representation of a single-phase Buck SMPS has been presented, where variations in the power rail components and parasitic resistances can be accommodated. With the analytical representation provided, numerical discretisation is avoided and robust digital control design techniques can be directly applied. Robust stability and feedback performance can be easily assessed using various robustness analysis algorithms. This modelling approach can be extended to different SMPS topologies, and this is the focus of future work.

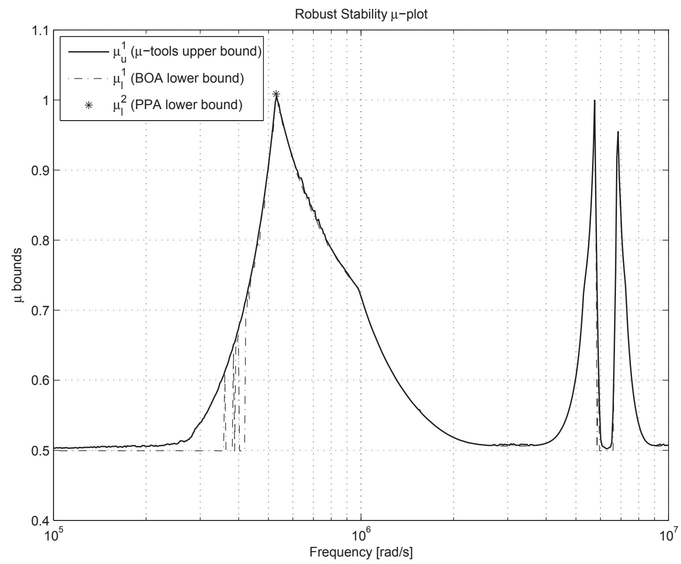

Fig. 5. Robustness Analysis Results.

REFERENCES

G. Balas, R. Chiang, A. Packard, and M. Safonov. *Robust Control Toolbox, User's Guide.* The MathWorks Inc, Natick, Massachusetts, 2010.

B. R. Barmish, P. P. Khargonekar, Z. C. Shi, and R. Tempo. Robustness margin need not be a continuous function of the problem data. *Systems and Control Letters*, 15:91–98, 1990.

R. Braatz and M. Morari. μ sensitivities as an aid for robust identification. In *Proceedings of the Amercian Control Conference*, pages 231–236, 1991.

J. Bu, M. Sznaier, Z. Q. Wang, and I. Batarseh. Robust controller design for a parallel resonant converter using μ-synthesis. *IEEE Transactions on Power Electronics*, 12:837–853, 1997.

J. C. Doyle. Analysis of feedback systems with structured uncertainties. In *IEE Proceedings*, volume 129(6), pages 242–250, 1982.

J. C. Doyle, A. Packard, and K. Zhou. Review of LFTs, LMIs and μ. In *Proceedings of the IEEE Conference on Decision and Control*, pages 1227–1232, Brighton, England, 1991.

R. Erickson and D. Maksimović. *Fundamentals of Power Electronics.* Springer (2nd edition), 2001.

M. Halton, M. Sharrer, and T. Scanlan. Application of the discrete-time structured singular value for dc-dc converters. In *Proceedings of the Irish Signals and Systems Conference*, Galway, Ireland, 2008.

M. J. Hayes and P. Iordanov. On the conservatism of the structured singular value as a basis for the construction of a robust root locus. In *Proceedings of the Irish Signals and Systems Conference*, pages 289–296, Dublin, Ireland, 2000.

P. Iordanov, M.J. Hayes, and M. Halton. On μ-analysis and synthesis for systems subject to real uncertainty. In *Proceedings of the European Control Conference*, Cambridge, UK, 2003.

D. Maksimović and R. Zane. Small-signal discrete-time modeling of digitally controlled pwm converters. In *Proceedings of the IEEE Transactions of Power Electronics*, pages 2552–2556, 2007.

J. A. Rossiter. *Model-Based Predictive Control - A Practical Approach.* CRC Press, 2003.

R. Sanchez-Peña and M. Sznaier. *Robust Systems Theory and Applications.* Wiley, 1998.

Appendix A. DISCRETE STATE SPACE MATRICES

$$
\Gamma_\Delta = \begin{bmatrix}
0 & w_L \\
0 & w_L \\
\dfrac{-(T_s - t_d)}{w_L^{-1} C_0} & -w_L + \dfrac{w_L \left(R_{C_0} + R_{L_0} \right) (T_s - t_d)}{L_0} \\
0 & w_L \\
\dfrac{w_C}{R_0} & 0 \\
-w_C & 0 \\
-w_C (T_s - t_d) & 0 \\
w_R & 0 \\
0 & \dfrac{-w_{R_L} R_{L_0}}{L_0} \\
0 & \dfrac{-w_{R_L} R_{L_0} (T_s - t_d)}{L_0} \\
0 & \dfrac{-w_{R_C} R_{C_0}}{L_0} \\
0 & \dfrac{-w_{R_C} R_{C_0} (T_s - t_d)}{L_0}
\end{bmatrix}^T
$$

$$
C_\Delta = \begin{bmatrix}
\dfrac{T_s}{L_0} & 0 \\
0 & \dfrac{\left(R_{C_0} + R_{L_0} \right) T_s}{L_0} \\
0 & 0 \\
0 & 0 \\
\dfrac{T_s}{C_0} & 0 \\
0 & \dfrac{T_s}{C_0} \\
0 & 0 \\
\dfrac{T_s}{R_0 C_0} & 0 \\
0 & T_s \\
0 & 0 \\
0 & T_s \\
0 & 0
\end{bmatrix}
$$

$$
D_{11} = \begin{bmatrix}
-w_L & 0 & 0 & 0 & 0 & 0 & 0 & 0 & 0 & 0 & 0 & 0 \\
0 & -w_L & 0 & 0 & 0 & 0 & 0 & 0 & \dfrac{w_{R_L} R_{L_0}}{L_0} & 0 & \dfrac{w_{R_C} R_{C_0}}{L_0} & 0 \\
0 & 0 & -w_L & 0 & 0 & 0 & 0 & 0 & 0 & 0 & 0 & 0 \\
0 & 0 & \dfrac{-\left(R_{C_0} + R_{L_0} \right)}{w_L^{-1} L_0 (T_s - t_d)^{-1}} & -w_L & 0 & 0 & 0 & 0 & 0 & \dfrac{R_{L_0} (T_s - t_d)}{w_{R_L}^{-1} L_0} & 0 & \dfrac{R_{C_0} (T_s - t_d)}{w_{R_C}^{-1} L_0} \\
0 & 0 & 0 & 0 & -w_C & 0 & 0 & 0 & 0 & 0 & 0 & 0 \\
0 & 0 & 0 & 0 & 0 & -w_C & 0 & 0 & 0 & 0 & 0 & 0 \\
0 & 0 & \dfrac{-w_L}{C_0} & 0 & 0 & 0 & -w_C & 0 & 0 & 0 & 0 & 0 \\
0 & 0 & 0 & 0 & \dfrac{-w_C}{R_0} & 0 & 0 & -w_R & 0 & 0 & 0 & 0 \\
0 & 0 & 0 & 0 & 0 & 0 & 0 & 0 & 0 & 0 & 0 & 0 \\
0 & 0 & -w_L & 0 & 0 & 0 & 0 & 0 & 0 & 0 & 0 & 0 \\
0 & 0 & 0 & 0 & 0 & 0 & 0 & 0 & 0 & 0 & 0 & 0 \\
0 & 0 & -w_L & 0 & 0 & 0 & 0 & 0 & 0 & 0 & 0 & 0
\end{bmatrix}
$$

$$
D_{12} = \begin{bmatrix} 0 & 0 & \dfrac{V_g T_s}{L_0} & \dfrac{V_g T_s \left(R_{C_0} + R_{L_0} \right) (T_s - t_d)}{L_0^2} & 0 & 0 & \dfrac{V_g T_s}{L_0 C_0} & 0 & 0 & \dfrac{V_g T_s}{L_0} & 0 & \dfrac{V_g T_s}{L_0} \end{bmatrix}^T
$$

$$
D_{21} = \begin{bmatrix} 0 & 0 & 0 & 0 & 0 & 0 & 0 & 0 & 0 & 0 & \dfrac{w_{R_C} R_{C_0}}{T_s} & 0 \end{bmatrix}
$$